J Electroceram (2009) 23:361–366
DOI 10.1007/s10832-008-9468-4

Electrical, optical, and structural properties of ITO co-sputtered IZO films by dual target magnetron sputtering

Jin-A Jeong · Kwang-Hyuk Choi · Jung-Hyeok Bae · Jong-Min Moon · Soon Wook Jeong · Insoo Kim · Han-Ki Kim · Min-Su Yi

Received: 4 June 2007 / Accepted: 28 February 2008 / Published online: 15 March 2008

Abstract We have investigated electrical, optical, and structural properties of indium tin oxide (ITO) co-sputtered indium zinc oxide (IZO) film prepared by a dual target direct current (DC) magnetron sputtering at room temperature in pure Ar ambient. It was shown that the resistivity and sheet resistance of ITO co-sputtered IZO films monotonically increased with increasing DC power of ITO target at constant DC power of IZO target. Synchrotron X-ray scattering and scanning electron microscope examination results show that addition of ITO in the IZO film lead to crystallization of IZTO film due to low transition temperature of the ITO from amorphous to crystalline. However, ITO co-sputtered IZO film (ITO/IZO power= 100 W:100 W) exhibit higher work function than those of pure IZO and ITO film. It was found that the work function as well as the electrical, optical, and surface properties of the IZTO film could be controlled by varying the DC power of IZO and ITO targets, respectively.

Keywords Co-sputtered IZO · ITO · IZTO · Work function · DC magnetron sputter

J.-A. Jeong · K.-H. Choi · J.-H. Bae · J.-M. Moon · S. W. Jeong · I. Kim · H.-K. Kim (✉)
School of Advanced Materials and Systems Engineering,
Kumoh National Institute of Technology (KIT),
1 Yangho-dong,
Gumi, Gyeongbuk 730-701, South Korea
e-mail: hkkim@kumoh.ac.kr

M.-S. Yi
Department of Materials Science and Engineering,
Kyoungbuk National University,
Sangju, Gyeongbuk 742-711, South Korea

1 Introduction

To fabricate high performance of flat panel displays and photovoltaics (PVs), it is necessary to obtain high-quality transparent conducting oxides (TCOs) films with high conductivity and transmittance in a visible spectra range. Therefore, there have been many efforts for developing TCO films with low resistivity, high transmittance, good adhesion, and good chemical stability [1–4]. Among many TCO materials, DC or RF sputtered indium tin oxide (ITO) films have been widely used in flat panel displays and PVs, due to their high conductivity and transmittance in a visible spectra range [5]. However, recent advance of new displays, such as organic light emitting diodes (OLEDs), flexible displays and organic based PVs require improvements in electrical and optical properties of ITO film used as transparent electrode [6–8]. In particular, imperfect work function alignment with a typical organic layer for hole injection or extraction requires a TCO film with high work function above 5 eV [9]. For this purpose, multi-component oxide films have been extensively explored as alternatives to conventional ITO film. Among the various muticomponent TCO materials, indium zinc tin oxide (IZTO) films have recently been recognized an alternative electrode material, due to their high work function (6.1 eV), good conductivity, high transparency, and low deposition temperature [10–14]. Furthermore, cosubstitutional of In_2O_3 by ZnO and SnO_2 raised the solubility due to isovalent substitution of a Sn^{4+} and Zn^{2+} cation for a pair of In^{3+} [12]. Phillips et al., reported that IZTO film prepared by pulsed laser deposition has conductivity within the ranges typically reported for ITO films [10]. In addition, Marks et al., in an investigation of the high work function transparent conducting oxide as an anode for an OLED, reported that an IZTO film has a higher work function (~6.1 eV) than a

commercial ITO (~4.7 eV) [14, 15]. Ambrosini et al. also reported a conductivity of 2,500 S/cm in $In_{2-2x}Sn_xZn_xO_{3-\delta}$ bulk pellet [12]. Although electrical and optical characteristics of the IZTO films prepared from IZTO target have reported, characteristics of IZTO films prepared by co-sputtering of conventional ITO and IZO targets have not been investigated in detail.

In this work, we have investigated the electrical, optical, structural, and surface properties of the ITO co-sputtered IZO film on glass substrate as a function of ITO DC power at constant IZO DC power. Using co-sputtering of commercial ITO and IZO target with low Sn and Zn content, we can easily control composition of the dopants (Zn, Sn) in the IZTO film. Even though low deposition temperature, the ITO co-sputtered IZO films show conductivity, transparency, and work function similar to those of a conventional ITO films. Based on synchrotron X-ray scattering, scanning electron microscope (SEM), Hall measurement analysis, and UV/Visible spectrometer analysis, we suggested a possible mechanism to describe ITO co-sputtering effect on characteristics of the IZTO film.

2 Experimental

A 150 nm-thick IZTO film was sputtered on a glass substrate by means of a dual target magnetron DC sputtering system at room temperature in a pure Ar ambient without the addition of reactive oxygen gas. Both IZO (5 wt.% ZnO doped In_2O_3) and ITO (5 wt.% SnO_2 doped In_2O_3) targets were used as co-sputtering target and were placed 100 mm from the glass substrate center. At constant DC power of IZO target (100 W), 150 nm-thick IZTO film were grown on a glass substrate with a dimension of 25× 25 mm as a function of ITO DC power. The IZO films (DC 100 W) were simultaneously co-sputtered with ITO target at DC power which ranged from 0 to 100 W. In addition, Ar flow rate and working pressure are maintained constant at 20 sccm and 5 mTorr during co-sputtering of IZO and ITO target. For simplicity, IZTO film co-sputtered at ITO DC power of 20 W is referred to as '20 W-IZTO' and so on. A schematic of the co-sputtering system used to deposit ITO co-sputtered IZO films is shown in Fig. 1 with the picture of plasma on IZO and ITO target during co-sputtering process. For uniform co-sputtering of IZO and ITO target, we employed a tilted magnetron gun as shown in Fig. 1. The deposition rate of the ITO co-sputtered IZO films was obtained by means of a stylus profilometer (Tencor Alpha-step 250). The sheet resistance and resistivity of the ITO co-sputtered IZO films were measured by four-point probe and Hall measurement with van der Pauw geometry at room temperature, respectively. The optical transmittance of the ITO co-sputtered IZO films was measured in the wavelength range from 220 to 800 nm by a UV/Visible spectrometer. The structural properties of the ITO co-sputtered IZO films were investigated by X-ray θ–2θ diffraction (XRD) measurements. A synchrotron X-ray scattering examinations were carried out at beamline 5C2 of Pohang Light Source in Korea. The synchrotron X-ray was focused by a mirror and a double bounce Si (111) monochromator was used to monochromatize X-rays to the wavelength of 0.12398 nm. The extent of ITO incorporation into the IZTO films was characterized by Auger electron spectroscopy (AES) using a PHI 670 Auger microscope with an electron beam of 10 keV and 0.0236 μA. The work functions of the ITO co-sputtered IZO films were measured by photoelectron spectroscopy with a UV source (PKI Model AC-2) at atmospheric pressure after surface ozone treatment. Furthermore, the surface morphology of the ITO co-sputtered IZO films was analyzed by SEM and atomic force microscopy (AFM).

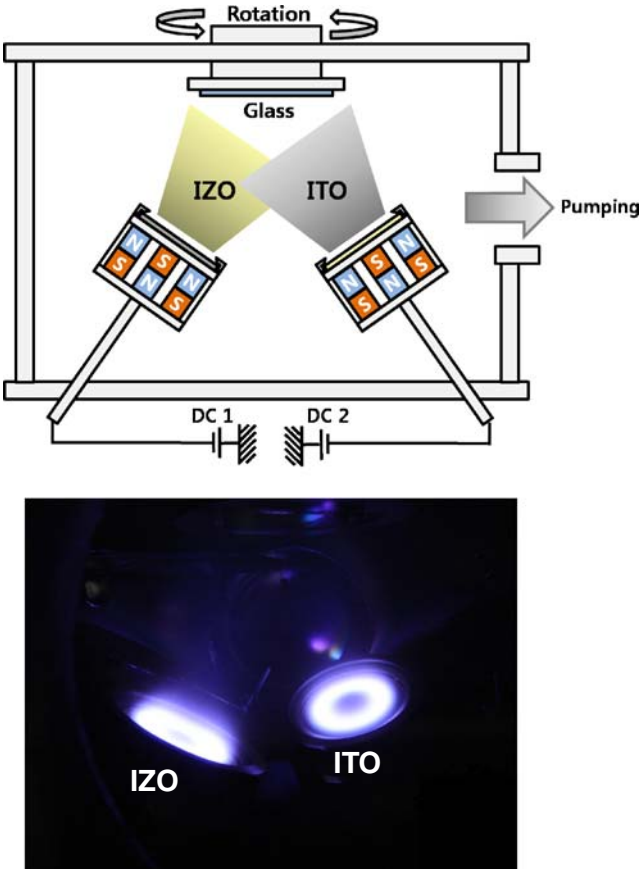

Fig. 1 Schematic figure of dual target DC sputtering system used for IZO and ITO co-sputtering and plasma picture during co-sputtering process

3 Results and discussion

The deposition rate of the IZTO films with increasing ITO DC power from 0 to 100 W is shown in Fig. 2. During co-

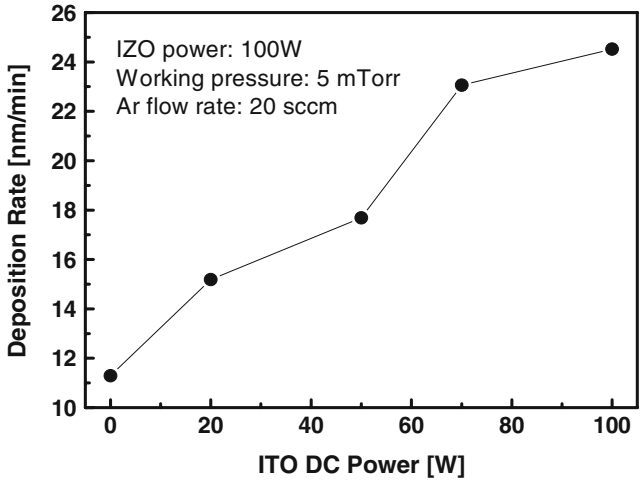

Fig. 2 Deposition rate of ITO co-sputtered IZO films on glass substrate with increasing ITO DC power at constant IZO DC power (100 W)

sputtering of ITO and IZO targets, the IZO DC power, working pressure, and Ar flow rate were maintained constant at 100 W, 5 mTorr, and 20 sccm, respectively. It was shown that the increase of ITO DC power resulted in a remarkable increase in deposition rate of the IZTO film. Increasing the ITO DC power to 100 W led to an increase in the deposition rate up to 24.5 nm min^{-1}.

Figure 3 shows the sheet resistance and resistivity of the IZTO film as a function of ITO DC power at a constant deposition condition and thickness (~150 nm). Both sheet resistance and resistivity of IZTO film significantly increased with an increase of ITO DC power at room temperature. Minami also reported that the resistivity of co-sputtered $Zn_2In_2O_5$–$In_4Sn_3O_2$ film monotonically increase with increasing RF power of the $In_4Sn_3O_2$, which is similar to our results [2]. Compared to pure IZO film (~3.4×10^{-4} Ω cm), ITO co-sputtered IZO films show higher resistivity (5.3×10^{-4}~1.7×10^{-3} Ω cm) due to high resistivity of ITO component. As increasing ITO DC power, more Sn atoms are incorporated into the IZTO film. However, it is thought that the Sn atoms in the IZTO film can not act as effective dopants at low substrate temperature. Hence, IZTO film exhibits higher resistivity with increasing ITO incorporation.

The optical transmittance of the ITO co-sputtered IZO films on glass substrate as a function of ITO DC power is shown in Fig. 4. It is clearly shown that the transmittance of the co-sputtered IZTO films is fairly high even though it is prepared at room temperature without oxygen reactive gas. It was noteworthy that the ITO co-sputtered IZO film exhibited higher transmittance than pure IZO film (83.5%) at 550 nm wavelength. The optical transmittance of 20, 50, 70 and 100 W-IZTO films at 550 nm is 83.8%, 87.0%, 89.0%, and 86.6%, respectively. Although the transmittance of IZO-based TCO in the UV region is lower than that of the ITO film, the average optical transmittance in visible region is comparable to that of conventional ITO films. From the view point of low temperature process for the flexible OLEDs and flexible PVs, ITO co-sputtered IZO film with high transmittance is the preferred TCO materials because they can be simply obtained at room temperature.

In order to examine the dependence of ITO co-sputtering on the microstructure of IZO films, synchrotron X-ray scattering analysis was performed. Figure 5 shows synchrotron X-ray results of the ITO co-sputtered IZO film with increasing ITO DC power at constant IZO power (100 W), working pressure (5 mTorr), and Ar flow rate (20 sccm). Synchrotron X-ray scattering result of 0 W-IZTO exhibits a broad peak (Q_z 2.05~2.4), indicating a completely amorphous structure. The stable amorphous phase of IZO film at room temperature unlike conventional ITO film can be explained by low kinetics of phase separation of ZnO and In_2O_3 for crystallization [4]. For the ITO co-sputtered IZO film (IZTO), however, additional

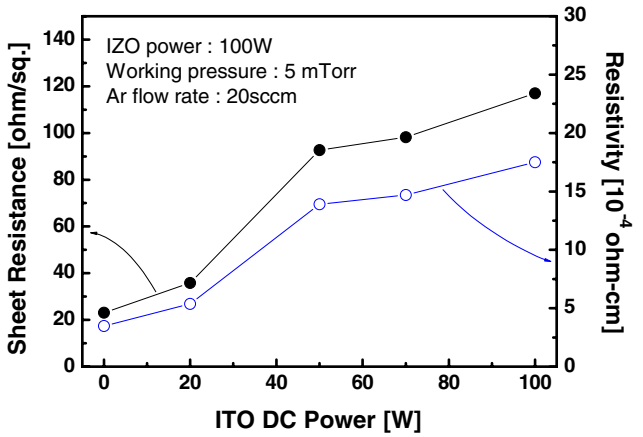

Fig. 3 Sheet resistance and resistivity of ITO co-sputtered IZO films with thickness of 150 nm as a function of ITO DC power

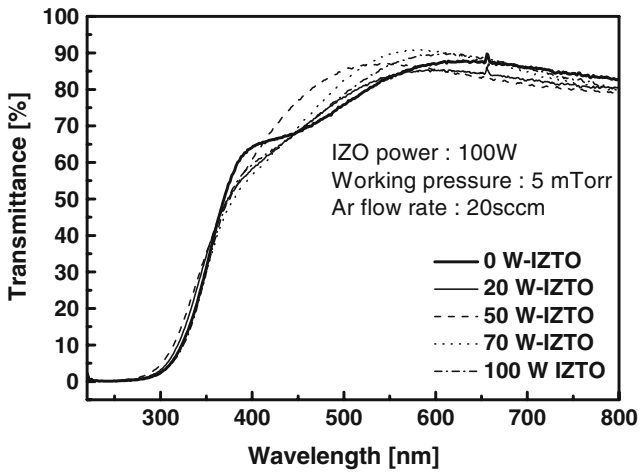

Fig. 4 Comparison of optical transmittance spectra obtained from ITO co-sputtered IZO films as a function of ITO DC power

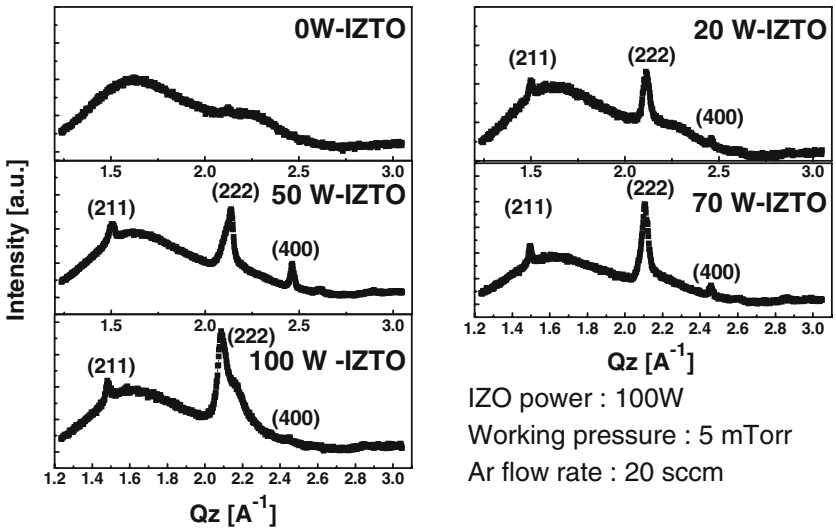

Fig. 5 Synchrotron X-ray scattering results of ITO co-sputtered IZO films as a function of ITO DC power

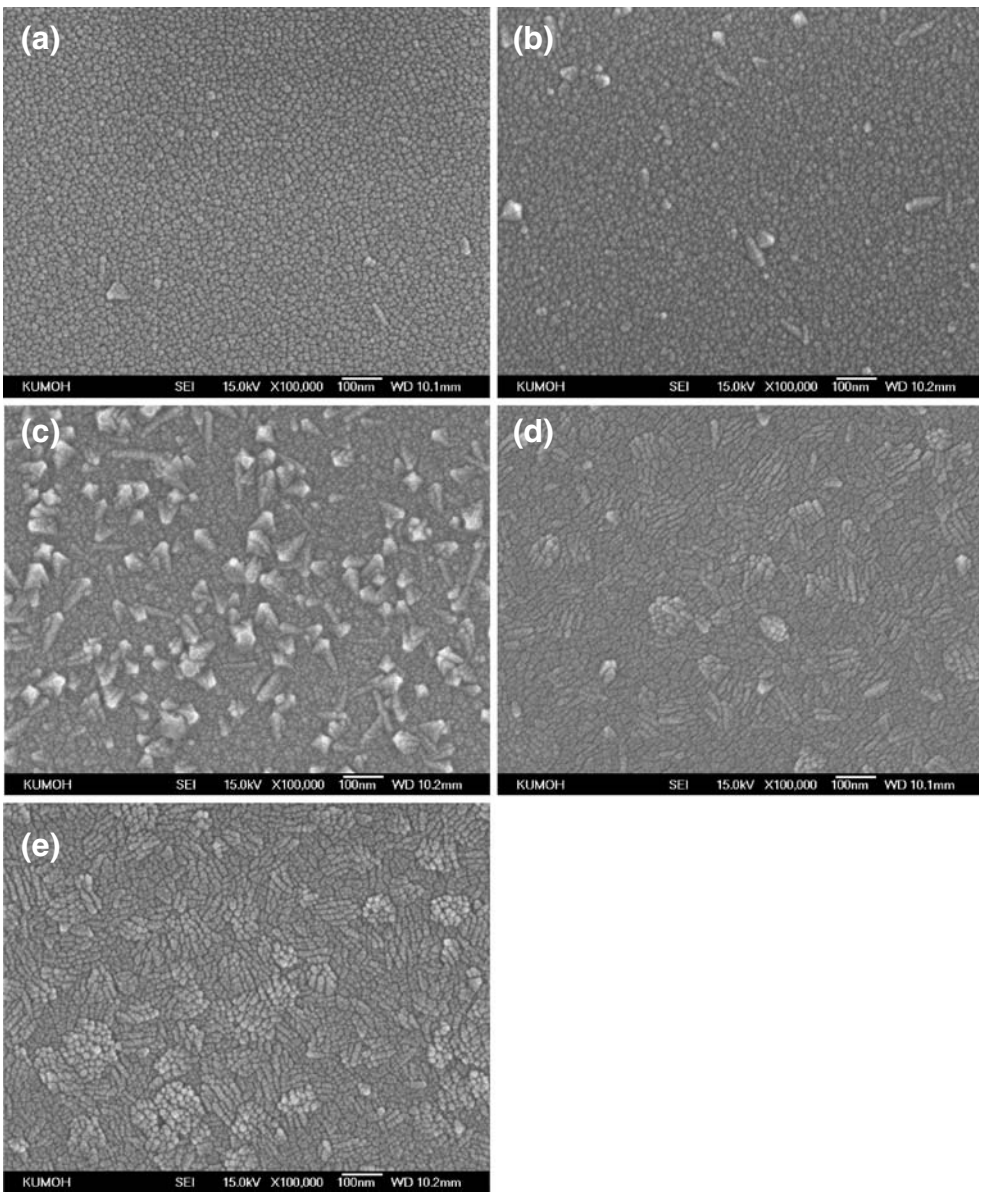

Fig. 6 Surface SEM images of ITO co-sputtered IZO films as a function of ITO DC power. (**a**) 0, (**b**) 20, (**c**) 50, (**d**) 70, and (**e**) 100 W-IZTO

peaks are observed at Q_z=1.49 (211), 2.11 (222), and 2.46 (400) peaks regardless of ITO DC power. This indicates that the ITO co-sputtering lead to the crystallization of the IZTO film. All IZTO films regardless of ITO DC power are polycrystalline structure with (222) dominant orientation. In addition, it was found that the intensity of (222) peak in the IZTO film increased with increasing ITO DC power from 20 to 100 W. In general, a conventional ITO film prepared by DC or RF sputtering has polycrystalline structure due to low amorphous/crystalline transition temperature (T/T_m< 0.19~150°C) [16]. Therefore, it is thought that the polycrystalline properties of IZTO film is caused by co-sputtered ITO component in the IZTO film.

The change in surface morphology in the ITO co-sputtered IZO film with increasing ITO DC power was examined by SEM and AFM analysis. SEM surface image of ITO co-sputtered IZO film with increasing ITO DC power was presented in Fig. 6. It was shown that the surface of the 0 W-IZTO film is smooth without defects such as pinhole and cracks. However, addition of ITO into the IZO films is found to lead to an increase in surface morphology of the IZTO film. In case of 0 W-IZTO films, very low root mean square (RMS) roughness (~0.8 nm) is measured by AFM analysis as shown in Fig. 7. However, 20 W-IZTO film reveals remarkable increase in RMS roughness of ~3.56 nm even though the SEM surface image is similar to that of the 0 W-IZTO film. In particular, the 50 W-IZTO film has a rough surface with a highest root mean square (RMS) roughness of 6.6 nm due to crystallization of ITO components as shown in Fig. 6(c). Further increase of ITO DC power resulted in a crystalline surface of the IZTO films as shown in Fig. 6(d) and (e), which is consistent with synchrotron X-ray scattering results. SEM surface images of both 70 and 100 W-IZTO film are similar to that of conventional crystalline ITO film due to severe crystallization of ITO component in the IZTO films. However, it was shown that the RMS roughness of the 70 and 100 W-IZTO films is lower than that of 50 W-IZTO film in Fig. 7.

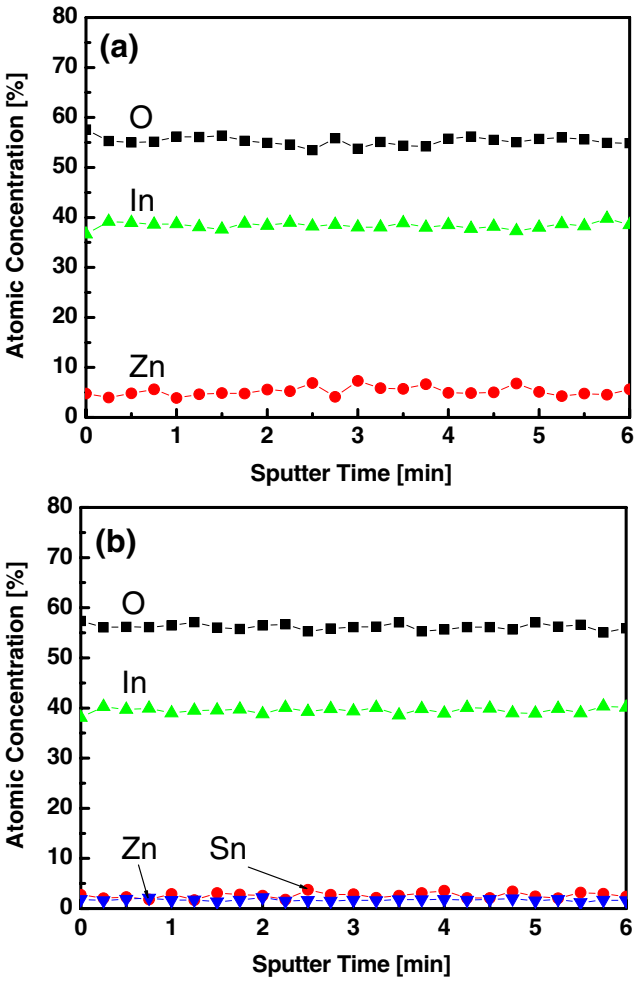

Fig. 8 AES depth profile results of (**a**) 0 and (**b**) 100 W-IZTO films

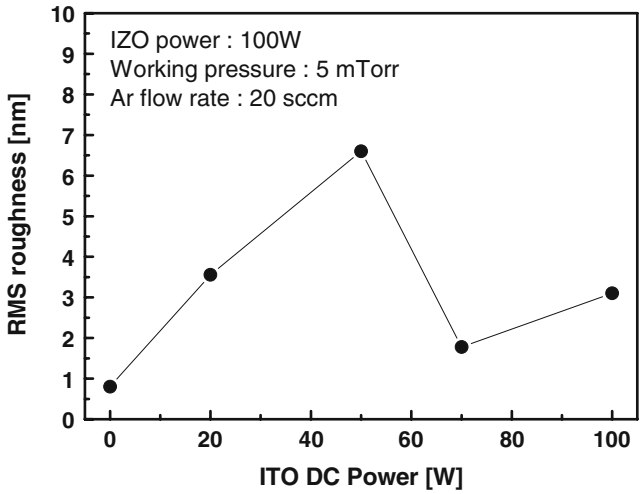

Fig. 7 Root mean square roughness of ITO co-sputtered IZO films as a function of ITO DC power

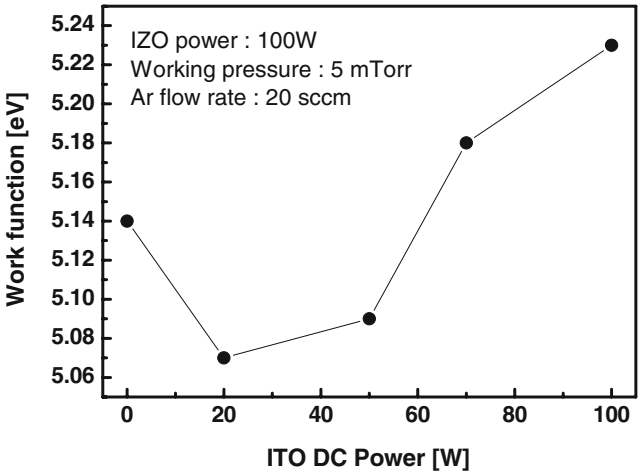

Fig. 9 Work function of ITO co-sputtered IZO film as a function of ITO DC power

Figure 8 shows the AES depth profiles of the 0 and 100 W-IZTO films. For the 0 W-IZTO film, the AES depth profiles result reveals a uniform distribution of O, In, and Zn, shown in Fig. 8(a). For the 100 W-IZTO film, however, it is evident that a small amount of Zn and Sn is incorporated into the IZTO film, shown in Fig. 8(b). It was also shown that O, In, Sn, and Zn atoms are uniformly distributed in the 100 W-IZTO film without variation of atomic concentration. This indicates that co-sputtering technique is a stable process to obtain multi-component TCO film. AES depth profiles of 20, 50, and 70 W-IZTO films (not shown here) are similar to that of 100 W-IZTO film due to low concentration of Zn and Sn dopants in the IZO and ITO targets.

To investigate the effect of ITO co-sputtering on work function of the IZTO film, photoelectron spectroscopy analysis at atmospheric pressure was employed. All IZTO samples were UV–ozone treated for 15 min to remove surface contamination and enhance work function. Figure 9 shows work function of the ITO co-sputtered IZO films as a function of ITO DC power. The work function of UV–ozone treated 0 W-IZTO film is 5.14 eV, which is higher value than that of conventional ITO film (4.5~5.0 eV). The ITO co-sputtering with 20 and 50 W DC power resulted in a decrease in work function lower than that of IZO film. However, it is noteworthy that increasing ITO DC power to 70 and 100 W led to a remarkable increase in work function of the IZTO film up to 5.18 and 5.23 eV. To obtain high performance flexible OLEDs and PVs, it is very important to use TCO layer with high work function above 5 eV, because the hole injection or extraction is critically dependant on barrier height between TCO and organic materials. Therefore, ITO co-sputtered IZO film (70 and 100 W-IZTO) with high work function is beneficial to enhance hole injection or extraction in OLEDs and organic based PVs. However, the work function measured in this work from 70 and 100 W-IZTO film is lower than previously reported value by Marks et al. (~6.1 eV) [14, 15]. The discrepancy of the work function with the previously reported value may be caused by the difference in the stoichiometry of the IZTO films and the method of preparation.

4 Summary and conclusion

Electrical, optical, structural, and surface properties of ITO co-sputtered IZO films on glass substrate were investigated by using, Hall measurement, UV/Visible spectrometer, synchrotron X-ray scattering, AES depth profile, and SEM examination, as a function of ITO DC power. It was found that addition of ITO into IZO resulted in crystallization and increase of resistivity of IZTO films. Although increase of ITO DC power resulted in increase of resistivity, co-sputtering of ITO with IZO could lead to an increase transmittance and work function of IZTO films. These findings show that the possibility of IZTO film with high work function as alternative TCO materials in flexible OLED and OPVs.

Acknowledgement This work was supported by Korea Research Foundation Grant funded by Korea Government (MOEHRD: Basic Research Promotion Fund) (KRF-2006-331-D00243).

References

1. D.D. Edwards, T.O. Mason, F. Gouenoire, K.R. Poeppelmeier, Appl. Phys. Lett. **70**, 1706 (1997)
2. T. Minami, J. Vac, Sci. Technol. A. **17**, 1765 (1999)
3. X. Jiang, F.L. Wong, M.K. Fung, S.T. Lee, Appl. Phys. Lett. **83**, 1875 (2003)
4. J.-H. Bae, J.-M. Moon, H.-K. Kim, J.-W. Kang, H.-D. Park, J.-J. Kim, W.J. Cho, J. Electrochem. Soc. **154**, 81 (2007)
5. R.B.H. Tahar, T. Ban, Y. Ohya, Y. Takahashi, J. Appl. Phys. **83**, 2631 (1998)
6. J.-W. Kang, W.-I. Jeong, J.-J. Kim, H.-K. Kim, D.-G. Kim, G.-H. Lee, Electrochem. Solid-State Lett. **10**, 75 (2007)
7. C.J. Brabec, N.S. Sariciftci, J.C. Hummelen, Adv. Func. Mater. **11**, 15 (2001)
8. H. Han, D. Adams, J.W. Mayer, T.L. Alford, J. Appl. Phys. **98**, 083705 (2005)
9. J.-M. Moon, J.-H. Bae, J.-A. Jeong, S.-W. Jeong, N.-J. Park, H.-K. Kim, J.-W. Kang, J.-J. Kim, M.-S. Yi, Appl. Phys. Lett. **90**, 163516 (2007)
10. J.M. Phillips, R.J. Cava, G.A. Thomas, S.A. Carter, J. Kwo, T. Siegrist, J.J. Krajewski, J.H. Marshall, W.F. Peck Jr., D.H. Rapkine, Appl. Phys. Lett. **67**, 2246 (1995)
11. T. Minami, T. Yamamoto, Y. Toda, T. Miyata, Thin Solid Films **373**, 189 (2000)
12. A. Ambrosini, S. Malo, K.R. Poeppelmeier, M.A. Lane, C.R. Kannewurf, T.O. Mason, Chem. Mater. **14**, 58 (2002)
13. N. Naghavi, C. Marcel, L. Dupont, C. Guery, C. Maugy, J.M. Tarascon, Thin Solid Films **419**, 160 (2002)
14. T.J. Marks, J.G.C. Veinot, J. Cui, H. Yan, A. Wang, N.L. Edleman, J. Ni, Q. Huang, P. Lee, N.R. Armstron, Synthetic Metals **127**, 29 (2002)
15. J. Cui, A. Wang, N.L. Edleman, J. Ni, P. Lee, N.R. Armstrong, T. J. Marks, Adv. Mater. **13**, 1476 (2001)
16. T. Oyama, N. Hashimoto, J. Shimizu, Y. Akao, H. Kojima, K. Aikawa, K. Suzuki, J. Vac. Sci. and Technol. A **10**, 1682 (1992)